



DØnote 4725-CONF

## Measurement of the Top Quark Mass in the Dilepton Channel

The DØ Collaboration  
URL <http://www-d0.fnal.gov>  
(Dated: February 25, 2005)

We present a preliminary measurement of the top quark mass in the dilepton channel based on about  $230 \text{ pb}^{-1}$  of data collected by the DØ experiment during Run II of the Fermilab Tevatron collider. We show that the method used obtains consistent results using ensemble tests of events generated with the DØ Monte Carlo simulation. We apply this technique to a total of 13 dilepton events selected in the collider data to obtain  $m_t = 155_{-13}^{+14}(\text{stat}) \pm 7(\text{syst}) \text{ GeV}$ .

*Preliminary Results for Winter 2005 Conferences*

## I. INTRODUCTION

We present a preliminary measurement of the top quark mass[1] based on about  $230 \text{ pb}^{-1}$  of data collected by the DØ experiment during Run II. The method used is similar to that used by the DØ Collaboration to measure the top quark mass in the dilepton channel using Run I data[2].

## II. THE DØ DETECTOR

The DØ detector is a typical multipurpose collider detector, that consists of central tracking, calorimeter, and muon detection systems.

The magnetic central-tracking system is comprised of a silicon microstrip tracker and a scintillating fiber tracker, both located within a 2 T superconducting solenoidal magnet [3]. Central and forward preshower detectors are located just outside of the coil and in front of the calorimeters. The liquid-argon/uranium calorimeter is divided into a central section covering  $|\eta| \leq 1$  and two end calorimeters extending coverage to  $|\eta| \leq 4$  [4]. In addition to the preshower detectors, scintillators between the calorimeter cryostats provide sampling of developing showers at  $1.1 < |\eta| < 1.4$ . The muon system is located outside the calorimeter and consists of a layer of tracking detectors and scintillation trigger counters before 1.8 T toroids, followed by two similar layers outside the toroids. Tracking at  $|\eta| < 1$  relies on 10 cm wide drift tubes [4], while 1 cm mini-drift tubes are used at  $1 < |\eta| < 2$ .

The trigger and data acquisition systems are designed to accommodate the high luminosities of Run II. Based on information from tracking, calorimeter, and muon systems, the output of the first level of the trigger is used to limit the rate for accepted events to  $\approx 1.5 \text{ kHz}$ . At the next trigger stage, with more refined information, the rate is reduced further to  $\approx 800 \text{ Hz}$ . These first two levels of triggering rely mainly on hardware and firmware. The third and final level of the trigger, with access to all the event information, uses software algorithms and a computing farm, and reduces the output rate to  $\approx 50 \text{ Hz}$ , which is written to tape.

## III. EVENT SELECTION

The event selection was developed for the measurement of the cross-section for  $t\bar{t}$ -production in the dilepton channel. We give a brief summary of the kinematic and topological selection cuts here. The analysis uses about  $230 \text{ pb}^{-1}$  of data from  $p\bar{p}$ -collisions at  $\sqrt{s}=1.96 \text{ TeV}$  collected with the DØ detector at the Fermilab Tevatron collider. In the  $e\mu$  channel, eight events were found that satisfy the requirements

- electron:  $p_T > 15 \text{ GeV}$ ,  $|\eta| < 1.1$  or  $1.5 < |\eta| < 2.5$ ;
- muon:  $p_T > 15 \text{ GeV}$ ;
- $\Delta R(e, \mu) > 0.25$ ;
- $\geq 2$  jets:  $p_T > 20 \text{ GeV}$ ,  $|\eta| < 2.5$ ;
- $\cancel{p}_T > 25 \text{ GeV}$ ;
- $\Delta\phi(\mu, \cancel{p}_T) > 0.25$ ;
- $H_T > 140 \text{ GeV}$ .

Here  $H_T$  is the scalar sum of the larger of the two lepton  $p_T$ s and all jet  $p_T$ s over 15 GeV. In the  $ee$  channel, five events were found that satisfy the requirements

- two electrons:  $p_T > 15 \text{ GeV}$ ,  $|\eta| < 1.1$  or  $1.5 < |\eta| < 2.5$ ;
- $\geq 2$  jets:  $p_T > 20 \text{ GeV}$ ,  $|\eta| < 2.5$ ;
- $m(ee) < 80 \text{ GeV}$  or  $m(ee) > 100 \text{ GeV}$ ;
- $\cancel{p}_T > \begin{cases} 40 \text{ GeV} & \text{if } m(ee) < 80 \text{ GeV} \\ 35 \text{ GeV} & \text{if } m(ee) > 100 \text{ GeV} \end{cases}$ ;
- sphericity  $> 0.15$ .

Table I gives the number of events that we expect to observe from the top-antitop quark signal and the background processes.

TABLE I: Expected event yield from background and signal processes.

process	$t\bar{t} \rightarrow e\mu$	$\gamma$ processes	$Z \rightarrow \tau\tau$	$WW/WZ$	$\mu$ +fake $e$	total
# events	$5.2\pm 0.6$	$0.02\pm 0.02$	$0.4\pm 0.1$	$0.4\pm 0.2$	$0.20\pm 0.06$	$6.2\pm 0.6$
process	$t\bar{t} \rightarrow ee$	$Z \rightarrow ee$	$Z \rightarrow \tau\tau$	$WW/WZ$	$e$ +fake $e$	total
# events	$1.9\pm 0.3$	$0.59\pm 0.09$	$0.13\pm 0.08$	$0.14\pm 0.09$	$0.07\pm 0.03$	$2.8\pm 0.3$

#### IV. ANALYSIS TECHNIQUE

As in the Run I publication[2], we follow the ideas proposed by Dalitz and Goldstein [5] to reconstruct events from decays of top-antitop quark pairs with two charged leptons (either electrons or muons) and two or more jets in the final state. Kondo has published similar ideas [6]. We use only the momenta of the two jets with the highest  $p_T$  in this analysis. We assign these two jets to the  $b$  and  $\bar{b}$  quarks from the decay of the  $t$  and  $\bar{t}$  quarks. We then assign a likelihood to hypothesized values of the top quark mass between 80 GeV and 280 GeV. For each event, we find the pairs of  $t$  and  $\bar{t}$  momenta that are consistent with the observed lepton and jet momenta and missing  $p_T$ . We call a pair of top-antitop quark momenta that is consistent with the observed event a solution. We assign a weight to each solution, given by

$$w = f(x)f(\bar{x})p(E_\ell^*|m_t)p(E_{\bar{\ell}}^*|m_t),$$

where  $f(x)$  is the parton distribution function for the proton for the momentum fraction  $x$  carried by the initial quark, and  $f(\bar{x})$  is the corresponding value for the initial antiquark. The quantity  $p(E_\ell^*|m_t)$  is the probability for the hypothesized top quark mass  $m_t$  that the lepton  $\ell$  has the observed energy in the top quark rest frame[5].

There are two ways to assign the two jets to the  $b$  and  $\bar{b}$  quarks. For each assignment of observed momenta to the final state particles, there may be up to four solutions for each hypothesized value of the top quark mass. The likelihood for each value of the top quark mass  $m_t$  is then given by the sum of the weights over all the possible solutions:

$$W_0(m_t) = \sum_{\text{solutions}} \sum_{\text{jets}} w_{ij}.$$

In this procedure we implicitly assume that all momenta are measured perfectly. The weight  $W_0(m_t)$  therefore is zero if no exact solution is found. However, the probability to observe this event if the top quark mass has the value  $m_t$  does not have to be zero if no exact solution is found, because of the finite resolution of the momentum measurements. We account for this by repeating the weight calculation with input values for the particle momenta that are drawn from normal distributions centered on the measured value with widths equal to the resolution of the momentum measurements. The missing  $p_T$  is corrected by the vector sum of the differences in the particle momenta from the measured values and an added random noise vector with  $x$  and  $y$ -components drawn from a normal distribution with a mean of zero and an rms of 8 GeV. We then average the weight curves obtained from  $N$  such variations:

$$W(m_t) = \frac{1}{N} \sum_{n=1}^N W_n(m_t).$$

We thus effectively integrate the weight  $W(m_t)$  over the final state parton momenta, weighted by the experimental resolutions. We refer to this procedure as resolution sampling.

For each event we use the value of the hypothesized top quark mass at which  $W(m_t)$  reaches its maximum as the estimator for the mass of the top quark. We call this mass value the peak mass. We cannot determine the top quark mass directly from the distribution of peak masses, because effects such as initial and final state radiation shift the most probable value of this distribution away from the actual top quark mass. We therefore generate the expected distributions of weight curve peaks for a range of top quark masses using Monte Carlo simulations. We call these distributions templates. Resolution sampling does not change the templates significantly. The rationale for employing resolution sampling is that it increases the number of events for which we find solutions. In Monte Carlo events with an input top quark mass of 175 GeV, about 10% of the events have no solutions as measured. After sampling 1000 times for each event the fraction of events without solutions drops to less than 1%.

We then compare the peak mass distribution of the observed events to these templates using a binned maximum likelihood fit. The likelihood is calculated as

$$L(m_t) = \prod_{i=1}^{n_{bin}} \left[ \frac{n_s s_i(m_t) + n_b b_i}{n_s + n_b} \right]^{n_i},$$

TABLE II: results of combined ensemble tests of 8  $e\mu$  and 5  $ee$  events drawn randomly from signal and background templates.

$m_t$	$\langle m_{fit} \rangle$	rms( $m_{fit}$ )	$\langle \text{pull} \rangle$	rms(pull)
140 GeV	141.5 GeV	13.2 GeV	-0.11	0.87
160 GeV	159.5 GeV	14.0 GeV	-0.09	0.93
175 GeV	176.3 GeV	15.1 GeV	-0.06	1.03
190 GeV	192.5 GeV	16.3 GeV	-0.21	1.10
210 GeV	211.1 GeV	14.0 GeV	-0.15	0.96

where  $n_i$  is the number of data events observed in bin  $i$ ,  $s_i(m_t)$  is the normalized signal template contents for bin  $i$  at top quark mass  $m_t$ ,  $b_i$  is the normalized background template contents for bin  $i$ . The product runs over all  $n_{bin}$  bins. The background template consists of events from all background sources added in the expected relative proportions. The signal-to-background fraction is fixed to  $n_s/n_b$  with the numbers of signal and background events ( $n_s$ ,  $n_b$ ) taken from Table I.

## V. PERFORMANCE WITH $D\bar{O}$ MONTE CARLO EVENTS

In order to demonstrate the performance of our method, we generate a large number of simulated experiments for several input top quark mass values. We refer to each of these experiments as an ensemble. We fit each of the ensembles to the templates as for the data. The distribution of measured top quark mass values from the ensemble fits gives an estimate of the parent distribution of our measurement.

Monte Carlo samples were generated for seven values of the top quark mass: 120, 140, 160, 175, 190, 210, and 230 GeV. The simulation uses ALPGEN[7] as the event generator, PYTHIA[8] for fragmentation and decay, and GEANT[9] for the detector simulation. Jet energy scale corrections (version 5.1) are applied and additional smearing is performed to adjust the resolutions to the values measured in the collider data. Figures 1-3 show the  $D\bar{O}$  Monte Carlo templates for three different top quark masses.

In order to fit the data sample we need to account for the effect of the background on the templates. We use  $t\bar{t}$ ,  $Z \rightarrow \tau\tau$ , and  $WW$  events generated with the full  $D\bar{O}$  Monte Carlo and fake electron events taken from the collider data sample. We add the background distributions from Figures 4-6 to the signal templates. The signal and background contributions are normalized to the expected signal-to-background ratio.

We perform ensemble tests in the two channels separately. A given event is taken from the signal and background samples with probabilities that correspond to the fraction of events expected from each sample. We also perform ensemble tests with 8  $e\mu$  and 5  $ee$  events combined. For the joint ensemble tests we calculate  $-\ln L$  at every mass point separately for the  $e\mu$  and the  $ee$  samples using the templates for the respective final state. Then we add  $-\ln L$  and fit the joint likelihood versus top quark mass. We use a cubic polynomial to fit the  $-\ln L$  points versus top quark mass. All points are included in the fit.

Table II lists the results of the joint ensemble tests and Figure 7 shows a plot of average fitted mass versus input top quark mass. These results indicate that the calibration curve is perfectly consistent with unit slope and zero offset. Thus our result is expected to be unbiased. The rms of the pulls are close to one, indicating that the error determined from the point at which  $-\ln L$  changes by half a unit gives an adequate estimate of the statistical uncertainty.

### A. Systematic Effects

The finite size of the Monte Carlo data samples limits the precision to which we can check the performance of the algorithm to about 1.3 GeV for the  $e\mu$  channel and to 2.2 GeV for the  $ee$  channel.

We use the ensemble test technique to study the effect of certain systematic effects. We make systematic changes to the events in the ensembles and fit them using the nominal templates. The change in the result gives the size of the systematic uncertainty.

Since we compare the results from the collider data against simulated templates, the measurement will be systematically biased if the jet energies are calibrated differently in data and simulation. The agreement between closure tests using collider data and simulated data is better than

$$\frac{\sigma_{jes}}{p_T} = \begin{cases} 5\% & p_T > 30 \text{ GeV} \\ 30\% - p_T/120 \text{ GeV} & p_T \leq 30 \text{ GeV} \end{cases}$$

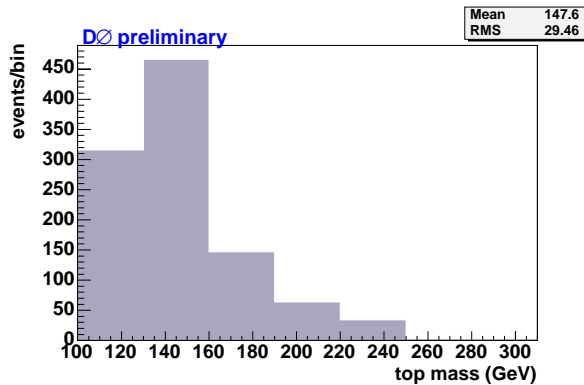


FIG. 1: Template from DØ Monte Carlo events from  $t\bar{t}$  decays for  $m_t=120$  GeV.

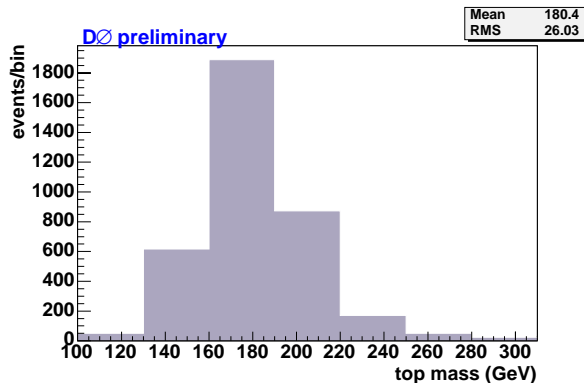


FIG. 2: Template from DØ Monte Carlo events from  $t\bar{t}$  decays for  $m_t=175$  GeV.

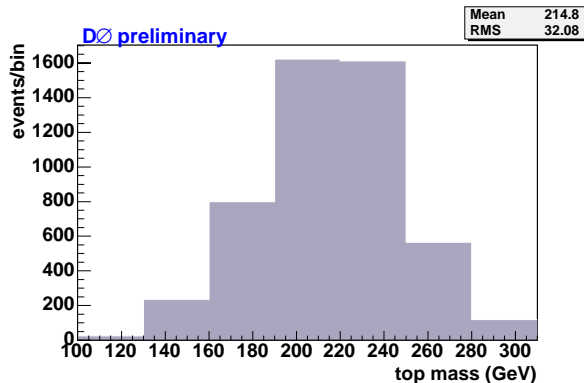


FIG. 3: Template from DØ Monte Carlo events from  $t\bar{t}$  decays for  $m_t=230$  GeV.

To estimate the effect of this uncertainty in the jet energy scale calibration, we generate ensembles with the jet  $p_{TS}$  increased and decreased by  $\sigma_{jes}$  and fit them with the nominal templates. We quote 5.6 GeV, half the difference between the two fits, as the systematic error.

In order to estimate the effect of the uncertainty in the background estimation on the result, we increase and decrease the expected signal-to-background ratio from Table I in the ensembles by one standard deviation while keeping the nominal templates. This corresponds to changing signal:background from 4.0 to 6.8 for the  $e\mu$  channel and from 1.6 to 2.5 for the  $ee$  channel. This results in a change of the average fitted mass of just below 1 GeV.

To estimate the effect of changes to the event generation we generate a large number of  $t\bar{t}$  decays with PYTHIA. We do not use the GEANT detector simulation here because the CPU time required exceeds available resources. In order to simulate the effects of jet reconstruction, we cluster all particles within a cone of  $\Delta R = \sqrt{(\Delta\phi)^2 + (\Delta\eta)^2}$

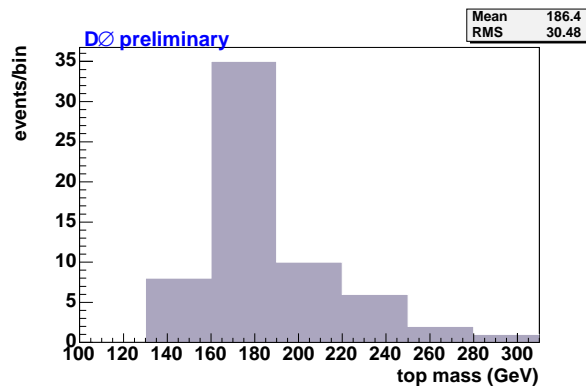


FIG. 4: Peak mass spectrum from DØ Monte Carlo for the  $Z \rightarrow \tau\tau$  background in the  $e\mu$  channel.

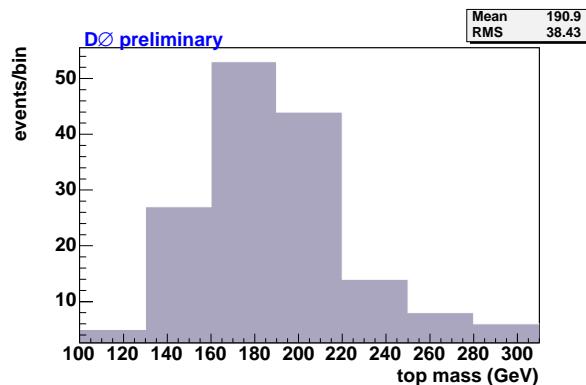


FIG. 5: Peak mass spectrum from DØ Monte Carlo for the  $WW \rightarrow e\mu$  background.

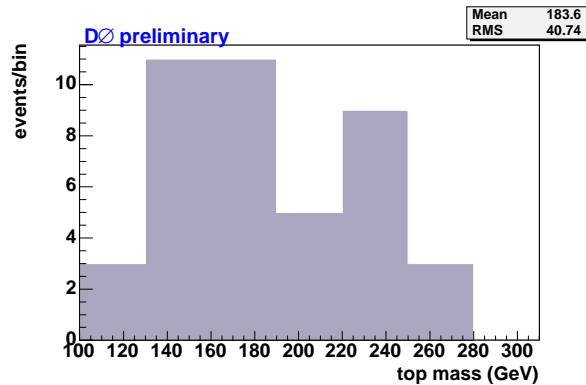


FIG. 6: Peak mass spectrum from data for the  $W + \text{jets} \rightarrow \mu + \text{fake } e$  background.

into one "jet". We generate samples of 10,000 events each with changed generation conditions and with 175 GeV top quark mass and fit them to nominal PYTHIA templates. The differences between the results of these samples and the nominal value of 175 GeV give estimates of the uncertainties due to these effects.

Turning off initial state radiation reduced the fitted mass by 1.5 GeV, turning off final state radiation increased the fitted mass by 4.6 GeV. The mass increased by 2.9 GeV if HERWIG[10] is used instead of PYTHIA and by 2.1 GeV if the next-to-leading order event generator MCNLO[11] is used. We set the uncertainty due to the event generator to  $\pm 3$  GeV. The variation between different parton distribution functions is 0.9 GeV.

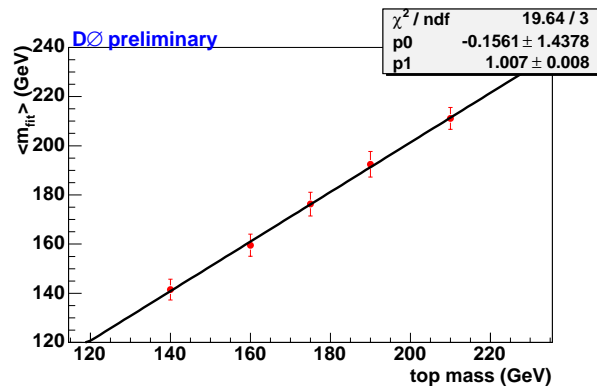


FIG. 7: Average fit mass versus input top quark mass for combined ensemble tests of 8  $e\mu$  and 5  $ee$  events. The error bars were inflated by a factor 10 to make them visible.

TABLE III: List of  $e\mu$  events. The columns give the measured transverse momenta of the electron, the muon, the two leading jets and the missing  $p_T$ . The last column gives the peak mass. All values are in GeV.

run	event	$p_T(e)$	$p_T(\mu)$	$p_T(j_1)$	$p_T(j_2)$	$\cancel{p}_T$	$m_{peak}$
168393	1997007	15.9	56.6	77.2	52.9	38.4	145
174901	8710859	136.5	29.6	88.5	87.9	84.4	269
177826	15259654	51.3	80.2	157.7	114.4	77.9	140
178159	37315438	109.3	123.4	65.5	46.0	40.7	133
178733	8735139	15.8	52.0	110.9	49.7	153.6	162
179141	11709332	30.5	52.5	57.3	41.5	30.0	164
179195	26386170	73.2	76.8	108.2	106.5	68.5	164
179331	19617819	39.1	39.3	124.5	79.0	29.1	214

## VI. RESULTS FROM COLLIDER DATA

The characteristics of the eight  $e\mu$  events found in the collider data sample are given in Table III. Figure 8 shows the weight curves. Table IV lists the  $ee$  events and the weight curves are shown in Figure 9.

We use the full  $D\bar{O}$  Monte Carlo templates and the nominal background contribution levels to fit the sample of eight  $e\mu$  events from Table III and the five  $ee$  events from Table IV. We measure  $m_t = 154^{+17}_{-15}$  GeV in the  $e\mu$  channel and  $m_t = 159^{+26}_{-22}$  GeV in the  $ee$  channel. The maximum of the joint likelihood occurs at  $155^{+14}_{-13}$  GeV (Figure 10). The statistical uncertainty obtained from the fit is consistent with expectations from ensemble tests as demonstrated in Figure 11.

We treat the systematic error due to Monte Carlo statistics as uncorrelated. All other systematic uncertainties are completely correlated between the two channels and the uncertainty on the combined result is the same as the uncertainty on the results from the individual channels. The statistical and systematic uncertainties are summarized in Table V and add in quadrature to a total uncertainty of 15 GeV.

The world average top quark mass measurement based on Run I data collected by CDF and  $D\bar{O}$  is  $m_t = 178.0 \pm 4.3$  GeV[12]. In order to estimate how consistent our result is with this value we perform ensemble tests with an input top quark mass of 175 GeV. In the  $e\mu$  channel, the fraction of ensemble tests that results in a measured mass of 154

TABLE IV: List of  $ee$  events. The columns give the measured transverse momenta of the two electrons, the two leading jets and the missing  $p_T$ . The last column gives the peak mass. All values are in GeV.

run	event	$p_T(e_1)$	$p_T(e_2)$	$p_T(j_1)$	$p_T(j_2)$	$\cancel{p}_T$	$m_{peak}$
166779	121971122	55.5	19.9	103.4	41.5	110.5	150
177681	13869716	67.4	58.7	82.7	34.3	43.9	144
178152	26229014	61.8	18.0	80.2	22.2	79.7	183
178177	13511001	97.6	18.9	128.5	52.3	98.7	192
180326	14448436	104.5	42.7	84.2	68.7	75.1	162

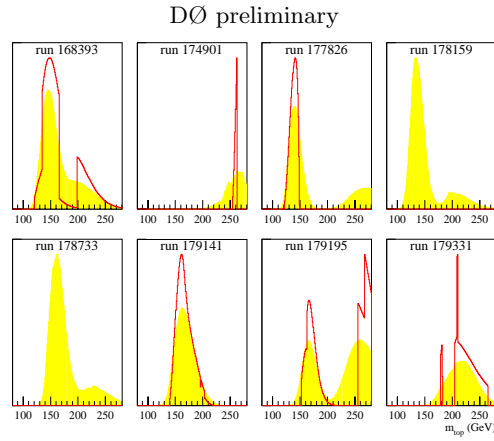


FIG. 8: Weight curves from the eight  $e\mu$  events in the collider data sample. The solid histograms show the weight curves with resolution sampling, the open histograms show the weight curves without resolution sampling.

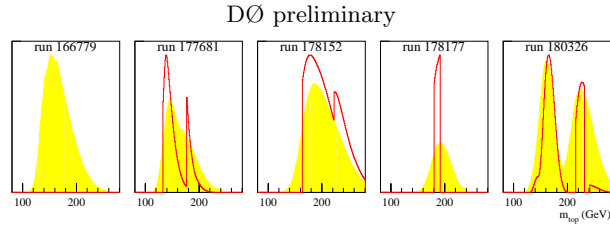


FIG. 9: Weight curves from the five  $ee$  events from the collider data sample. The solid histograms show the weight curves with resolution sampling, the open histograms show the weight curves without resolution sampling.

GeV or lower is 12%. In the  $ee$  channel the fraction of ensembles that give a result of 159 GeV or less is 26%. For the combined result there is an 8% probability to measure a value of 155 GeV or lower if the top quark mass is 175 GeV. The distribution of measured top quark masses for ensemble tests with 8  $e\mu$  events and 5  $ee$  events is shown in Figure 12.

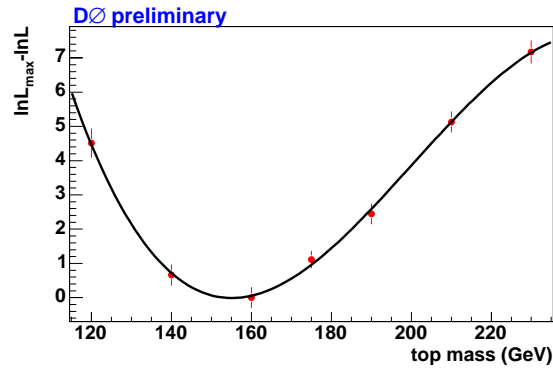


FIG. 10: Plot of  $-\ln L$  versus top quark mass for both channels combined.

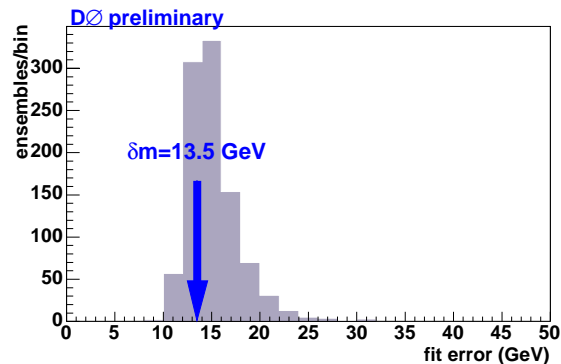


FIG. 11: Statistical uncertainties returned by fits to ensemble tests with 8  $e\mu$  and 5  $ee$  events generated with an input top quark mass of 175 GeV. The arrow indicates the uncertainty obtained from the fit to the collider data.

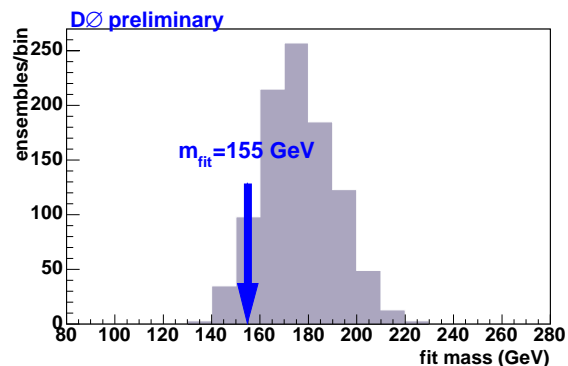


FIG. 12: Fit masses from ensemble tests for 8  $e\mu$  and 5  $ee$  events generated with an input top quark mass of 175 GeV. The arrow indicates the measured value.

## VII. CONCLUSION

In this paper we present a preliminary measurement of the top quark mass in the dilepton channel. We show that the method used obtains consistent results using ensemble tests of events generated with the DØ Monte Carlo simulation. We apply this technique to the eight  $e\mu$  events and five  $ee$  events found in the collider data. The best fit value for the top quark mass that we obtain is  $m_t = 155_{-13}^{+14}(\text{stat}) \pm 7(\text{syst})$  GeV. We obtain the total systematic uncertainty by adding all systematic uncertainties in quadrature. The statistical and systematic uncertainties add in quadrature to a total uncertainty of 15 GeV.

TABLE V: summary of uncertainties.

source	uncertainty
statistical	+14/-13 GeV
systematic	6.7 GeV
jet energy scale	5.6 GeV
event generation	3.0 GeV
parton distribution functions	0.9 GeV
underlying event simulation	1.0 GeV
background	1.0 GeV
calibration	1.1 GeV
total	15 GeV

### Acknowledgments

We thank the staffs at Fermilab and collaborating institutions, and acknowledge support from the Department of Energy and National Science Foundation (USA), Commissariat à l’Energie Atomique and CNRS/Institut National de Physique Nucléaire et de Physique des Particules (France), Ministry of Education and Science, Agency for Atomic Energy and RF President Grants Program (Russia), CAPES, CNPq, FAPERJ, FAPESP and FUNDUNESP (Brazil), Departments of Atomic Energy and Science and Technology (India), Colciencias (Colombia), CONACyT (Mexico), KRF (Korea), CONICET and UBACyT (Argentina), The Foundation for Fundamental Research on Matter (The Netherlands), PPARC (United Kingdom), Ministry of Education (Czech Republic), Canada Research Chairs Program, CFI, Natural Sciences and Engineering Research Council and WestGrid Project (Canada), BMBF and DFG (Germany), Science Foundation Ireland, A.P. Sloan Foundation, Research Corporation, Texas Advanced Research Program, Alexander von Humboldt Foundation, and the Marie Curie Fellowships.

- 
- [1] Sarosh N. Fatakia, Ph.D. thesis, Boston University 2005, unpublished.
  - [2] DØ Collaboration, Phys. Rev. Letters 80, 2063 (1998); Phys. Rev. D 60, 052001 (1999).
  - [3] DØ Collaboration, V. Abazov *et al.*, “The Upgraded DØ Detector”, in preparation for submission to Nucl. Instrum. Methods Phys. Res. A, and T. LeCompte and H.T. Diehl, Ann. Rev. Nucl. Part. Sci. **50**, 71 (2000).
  - [4] DØ Collaboration, S. Abachi *et al.*, Nucl. Instrum. Methods Phys. Res. A **338**, 185 (1994).
  - [5] R.H. Dalitz and G.R. Goldstein, Phys Rev. D 45, 1531 (1992).
  - [6] K. Kondo, J. Phys. Soc. Jpn. 57, 4126 (1988); 60, 836 (1991).
  - [7] M.L. Mangano, M. Moretti, F. Piccinini, R. Pittau, A. Polosa, JHEP 0307:001,2003, hep-ph/0206293; M.L. Mangano, M. Moretti, R. Pittau, Nucl.Phys.B632:343-362,2002; hep-ph/0108069; F. Caravaglios, M. L. Mangano, M. Moretti, R. Pittau, Nucl.Phys.B539:215-232,1999; hep-ph/9807570.
  - [8] T. Sjöstrand *et al.*, Computer Physics Commun. 135 (2001) 238.
  - [9] S. Agostinelli *et al.*, Nuclear Instruments and Methods in Physics Research A506, 250 (2003).
  - [10] G. Corcella, I.G. Knowles, G. Marchesini, S. Moretti, K. Odagiri, P. Richardson, M.H. Seymour, B.R. Webber, hep-ph/0011363.
  - [11] S. Frixione, P. Nason, B.R. Webber, JHEP08(2003)007.
  - [12] DØ Collaboration, Nature 429, 638 (2004).